New crystal structure and physical properties of TcB from first-principles calculations*

Zhang Gang-Tai(张刚台)[a)b)†], Bai Ting-Ting(白婷婷)[c)], Yan Hai-Yan(闫海燕)[d)‡], and Zhao Ya-Ru(赵亚儒)[a)]

[a)] College of Physics and Optoelectronics Technology, Baoji University of Arts and Sciences, Baoji 721016, China
[b)] School of Physics and Optoelectronic Technology, Dalian University of Technology, Dalian 116024, China
[c)] College of Mathematics and Information Science, Baoji University of Arts and Sciences, Baoji 721013, China
[d)] College of Chemistry and Chemical Engineering, Baoji University of Arts and Sciences, Baoji 721013, China

(Received 18 March 2015; revised manuscript received 24 May 2015; published online 20 August 2015)

By combining first-principles calculations with the particle swarm optimization algorithm, we predicted a hexagonal $P\bar{3}m1$ structure for TcB, which is energetically more favorable than the previously reported WC-type and *Cmcm* structures. The new phase is mechanically and dynamically stable, as confirmed by its phonon and elastic constants calculations. The calculated mechanical properties show that it is an ultra-incompressible and hard material. Meanwhile, the elastic anisotropy is investigated by the shear anisotropic factors and ratio of the directional bulk modulus. Density of states analysis reveals that the strong covalent bonding between Tc and B atoms plays a leading role in forming a hard material. Additionally, the compressibility, bulk modulus, Debye temperature, Grüneisen parameter, specific heat, and thermal expansion coefficient of TcB are also successfully obtained by using the quasi-harmonic Debye model.

Keywords: TcB, structure prediction, ultra-incompressible material, thermodynamic properities

PACS: 61.66.Fn, 61.50.Ah, 62.20.de **DOI:** 10.1088/1674-1056/24/10/106104

1. Introduction

Designing and searching for ultra-incompressible and superhard materials are of great scientific interests owing to their various industrial applications, such as cutting and polishing tools, abrasives, oil exploitations, and coatings. Generally, there are two kinds of materials that are regarded as potential candidates for superhard materials. One is the strong covalent-bonded compounds formed by light atoms, such as diamond,[1] *c*-BN,[2] B_6O,[3] BC_2N,[4] and BC_5.[5] The other is by combining heavy transition metal (TM) atoms with light and covalent bonding atoms, such as OsB_2,[6] ReB_2,[7] RuC,[8] ReN_4,[9] OsO_2,[10] etc. The compounds formed by transition metal and light atoms usually possess high valence electron density and directional covalent bonds, and these covalent bonds are strong enough to inhibit creation and movement of dislocations, which significantly improve their mechanical properities and create high hardness. In view of this point, recent design of the new intrinsically potential superhard materials has concentrated on light element TM compounds. A primary example and among the first synthesized materials following this principle is OsB_2,[6] which is expected to be a superhard material ($H_v \geq 40$ GPa). However, further calculations and experiments reveal that it is only a hard material.[11–13] Later, Yong *et al.*[14] synthesized OsN_2 at high pressures and temperatures, and the obtained zero-pressure bulk modulus was comparable with those of the traditional superhard materials. Many years earlier, Kempter and Nadler[15] claimed that they have synthesized WC-type OsC at ambient pressure and high temperature. No other experimental synthesis of osmium carbide has been reported since then. Recently, Guo *et al.*[16] investigated the structure and mechanical properties of OsC with nine structures and proposed that the synthesized OsC should be in NiAs structure. Liang *et al.*[17] systematically studied the electronic structure and mechanical properties of OsB, OsC, and OsN in the WC, NaCl, CsCl, and ZnS structures and also found that only four phases are mechanically stable but none of them is superhard. Very recently, Zhang *et al.*[18] reported an orthorhombic *Pmmn* structure for OsB_4 with high bulk modulus (294 GPa) and large hardness (28 GPa) energetically much superior to the previously reported WB_4-type structure.

Technetium (Tc) lies to the top left of Os in the periodic table, which should have a low compressibility, so it is worth studying the mechanical properties of its borides, carbides, and nitrides. Theoretically, technetium-based materials have been extensively studied.[19–25] For example, Wang[19] proposed the hexagonal structure of TcB_2 is more stable than the orthorhombic one and showed it is a potential superhard material. Liang *et al.*[20] reported that TcC and TcN in two hexagonal phases are ultra-incompressibile. Aydin and Simsek[21] investigated the structure, mechanical, and electronic proper-

*Project supported by the Science Foundation of Baoji University of Arts and Sciences of China (Grant No. ZK11061) and the Natural Science Foundation of the Education Committee of Shaanxi Province, China (Grant Nos. 2013JK0637, 2013JK0638, and 2014JK1044).

†Corresponding author. E-mail: gtzhang79@163.com
‡Corresponding author. E-mail: hyyan1102@163.com

© 2015 Chinese Physical Society and IOP Publishing Ltd

ities of TcB_2 and also showed that TcB_2 within ReB_2-type is energetically favorable than that of the AlB_2-type one and it is a hard material. Deligoz *et al.*[22] investigated the lattice dynamical and thermodynamical properties for TcB_2 in AlB_2, ReB_2, and OsB_2-type structures. Zhong *et al.*[23] studied the phase stability, physical properties, and hardness of TcB_2 in the ReB_2 and OsB_2 structures. Wu *et al.*[24] established the phase stability of technetium borides with various stoichiometries and also showed that the predicted *Cmcm* structure is more stable than the previously proposed WC-type structure.[25]

To the best of our knowledge, technetium monoboride (TcB) has not been experimentally synthesized so far due to the technical difficulty, besides, TMBs can be synthesized under ambient pressure, which leads to the low-cost synthesis condition and is beneficial to their applications. Because of this, in this paper we shall extensively investigate the ground-state structure of TcB by the *ab initio* particle swarm optimization (PSO) approach for crystal structure prediction.[26] This method has been successful in predicting crystal structures for various systems,[27–29] unbiased by any known information. A hexagonal $P\bar{3}m1$ structure is uncovered for TcB, which is energetically much superior to the previously proposed WC-type and *Cmcm* structures under ambient condition. The first principles calculations will be performed to study the total energy, lattice parameters, elastic modulus, and density of states for the novel hexagonal phase. In addition, the elastic anisotropy and the hardness are also determined. To further study TcB, the thermodynamic properties are also investigated by the quasi-harmonic Debye model.[30]

2. Computational details

The PSO methodology for crystal structural prediction has been implemented in the crystal structure analysis by the particle swarm optimization (CALYPSO) code[31] with 1∼4 formula units (f.u.) per simulation cell. The underlying calculations are performed using density functional theory within the generalized gradient approximation (GGA), as implemented in the Vienna *ab initio* simulation package (VASP).[32–34] The electron and core interactions are included by using the frozen-core all-electron projector augmented wave (PAW) method,[35] where the $2s^2 2p^1$ and $4p^6 4d^5 5s^2$ are considered as valence electrons for B and Tc, respectively. The cutoff energy 520 eV and proper Monkhorst–Pack k meshes $(14\times14\times6)$[36] are used to ensure that the total energy calculations are well converged to better than 1 meV/atom. The phonon frequency is calculated by using a supercell approach as implemented in the PHONOPY code.[37] Single crystal elastic constants are determined by the strain–stress method. The bulk modulus, shear modulus, Young's modulus, and Poisson's ratio are derived from the Voigt–Reuss–Hill approximation.[38] The quasi-harmonic Debye model is applied to study the lattice thermal expansion and the specific procedure of calculation can be found elsewhere.[30]

3. Results and discussion

At 0 GPa, a new stable structure with space group $P\bar{3}m1$ is predicted successfully, as shown in Fig. 1. The $P\bar{3}m1$ structure contains two TcB f.u. per one unit cell ($a_0 = b_0 = 2.871$ Å and $c_0 = 5.886$ Å), in which the Tc and B atoms occupy the Wyckoff 2d (0.3333, 0.6667, 0.314) and 2d (0.6667, 0.3333, 0.0606) sites, respectively. The bulk modulus (B_0) and its pressure derivative (B_0') are estimated by fitting the calculated total energy versus volume to the third-order Birch–Murnaghan equation of state (EOS),[39] and the corresponding results are $B_0 = 294$ GPa and $B_0' = 4.33$, respectively. Unfortunately, there are no available data for comparison. We hope that our results can provide powerful guidelines for further experimental and theoretical investigations. Figure 2 presents the dependences of the total energy on the f.u. volume for three different phases of TcB. As we expected, the $P\bar{3}m1$ structure for TcB has the lower energy minimum than the *Cmcm* and WC-type structures. This means that the $P\bar{3}m1$ structure is the ground-state phase at 0 GPa. At zero temperature, a stable crystalline structure requires all phonon frequencies to be positive. Thereby, we perform the phonon dispersion calculation for $P\bar{3}m1$-TcB at 0 GPa. As shown in Fig. 3, no imaginary phonon frequency appears in the whole Brillouin zone, indicating its dynamical stability. To study the thermodynamic stability for further experimental synthesis, the formation enthalpy of $P\bar{3}m1$-TcB with respect to the separate phases is quantified by the reaction route $\Delta H = H_{(\mathrm{TcB})} - H_{(\mathrm{Tc})} - H_{(\mathrm{B})}$. The hexagonal Tc and α-B[40] are chosen as the reference phases. The results obtained for $P\bar{3}m1$-TcB (−0.647 eV) in this reaction route have demonstrated the stability against the decomposition into the mixture of Tc and α-B. Compared with the WC-type (GGA: −0.51 eV)[25] and *Cmcm* (−0.63 eV)[24] phases, the $P\bar{3}m1$ phase possesses a lower formation enthalpy. Consequently, our predicted $P\bar{3}m1$ structure is easy to be synthesized at the ambient condition.

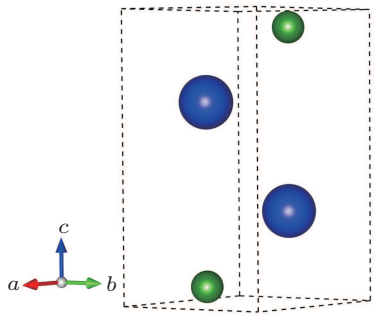


Fig. 1. (color online) Crystal structure of $P\bar{3}m1$-TcB. The big and small spheres represent Tc and B atoms.

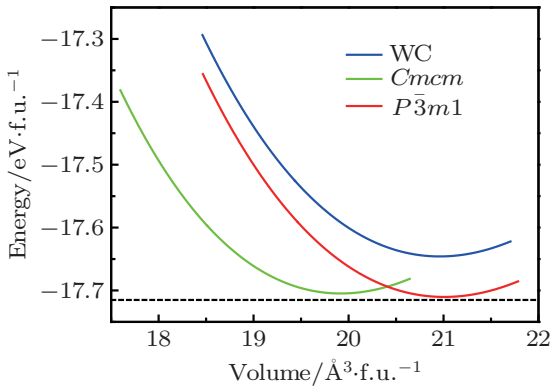


Fig. 2. (color online) Total energy versus f.u. volume for three different phases of TcB.

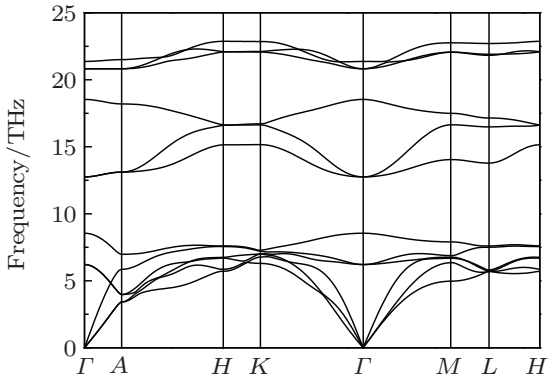


Fig. 3. Phonon dispersion curves of $P\bar{3}m1$-TcB at 0 GPa.

The mechanical properties of the $P\bar{3}m1$ phase are important for its potential technological and industrial applications. They define the behaviors of the solids that undergo stress, deform, and then recover and return to their original shapes after the stress ceases. By the strain–stress method, we have obtained the zero-pressure elastic constants C_{ij} of $P\bar{3}m1$-TcB and WC-TcB, which are listed in Table 1, together with the theoretical results of the other two phases of TcB. The elastic stability is a necessary condition for a stable crystal. For a stable hexagonal structure, C_{ij} should satisfy the following criteria:[41] $C_{33} > 0$, $C_{44} > 0$, $C_{12} > 0$, $C_{11} > |C_{12}|$, $(C_{11} + 2C_{12})C_{33} > 2C_{13}^2$. From Table 1, it can be seen that these conditions are satisfied completely, confirming that it is mechanically stable. It is also found that the $P\bar{3}m1$ phase has a larger C_{11} and C_{33} than the WC-type and *Cmcm* phases, reflecting that it is the a axis and c axis directions that are extremely stiff. The Young's modulus E and Poisson's ratio v can be derived by the equations $E = 9BG/(3B + G)$ and $v = (3B - 2G)/(6B + 2G)$. The calculated bulk modulus B, shear modulus G, Young's modulus E, and Poisson's ratio v of the $P\bar{3}m1$ phase together with the reference materials mentioned above are listed in Table 1. From Table 1, the bulk modulus of $P\bar{3}m1$-TcB is 290 GPa, which is higher than the experimental data of RuB (261 GPa)[42] but close to those of OsB_2 (343 GPa)[42] and ReB_2 (360 GPa),[7] indicating it is a potential ultra-incompressible material. Moreover, the obtained bulk modulus (B) is in good consistence with that (B_0) directly obtained from the fitting of the third-order Birch–Murnaghan EOS, further verifying the reliability of our elastic calculations. To compare the incompressibility of TcB in different phases under pressure, the volume compressions as a function of pressure are plotted in Fig. 4, in which the results of c-BN, OsB, and RuB are also given for reference. As shown in Fig. 4, TcB in the $P\bar{3}m1$, WC-type, and *Cmcm* phases has almost the same incompressibility due to their very close bulk moduli. Compared to the bulk modulus, the shear modulus of a material quantifies its resistance to the shear deformation and acts as a better indicator of the potential hardness. Fortunately, the $P\bar{3}m1$ phase has a large shear modulus of 206 GPa, thus it is expected to withstand the shear strain to a large extent. In addition, Poisson's ratio is a crucial parameter to describe the degree of directionality of the covalent bonding. The smallest Poisson's ratio (0.21) in the $P\bar{3}m1$ structure implies its strong degree of covalent bonding in three different phases for TcB. By using the empirical G–H_v or E–H_v relationships,[43] the estimated Vickers hardness for $P\bar{3}m1$-TcB is 30.3 GPa, which is comparable to the known hard materials of ReB_2 (32.9 GPa) and B_4C (32.8 GPa).[44] Furthermore, the Debye temperature links to many physical properties of materials such as elastic constants and melting temperature.[45] The Debye temperature can be estimated directly from the elastic constants. The obtained Debye temperature of $P\bar{3}m1$-TcB is 733 K, which is comparative to the values of the known ultra-incompressible RuB_2 (780 K),[46] ReN_2 (735 K),[47] and ReB_2 (858.3 K).[48] All of these excellent properties strongly support that $P\bar{3}m1$-TcB is an ultra-incompressible and hard material.

Table 1. Calculated elastic constants C_{ij} (GPa), bulk modulus B (GPa), shear modulus G (GPa), Young's modulus E (GPa), Poisson's ratio v, and B/G of $P\bar{3}m1$-TcB.

Structure	C_{11}	C_{12}	C_{13}	C_{22}	C_{33}	C_{44}	C_{55}	C_{66}	B	G	E	B/G	υ
$P\bar{3}m1$ (this work)	535	170	121		732	199		182	290	206	500	1.41	0.21
WC (this work)	511	170	195		617	216		170	305	191	474	1.6	0.24
WC (GGA)[25]	513	183	191		634	217		165	308	218	529	1.41	0.27
Cmcm[24]	467	258	199	344	523	113	210	135	300	133	348	2.26	0.31

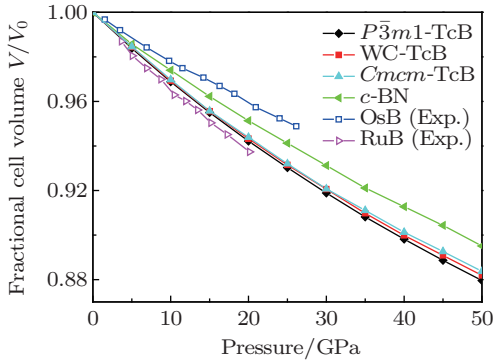


Fig. 4. (color online) Calculated volume compressions as a function of pressure for TcB in different phases compared with c-BN, OsB, and RuB.

The elastic anisotropy of crystals can exert great effects on the properties of the physical mechanism, such as anisotropic plastic deformation, crack behavior, and elastic instability. Therefore, it is important to study the elastic anisotropy to improve their mechanical durability. The shear anisotropic factors provide a measure of the degree of anisotropy in the bonding between atoms in different planes. For hexagonal $P\bar{3}m1$-TcB, the shear anisotropic factors for the $\{100\}$ shear planes between the $\langle 011\rangle$ and $\langle 010\rangle$ directions and for the $\{010\}$ shear planes between the $\langle 101\rangle$ and $\langle 001\rangle$ directions are defined as $A_1 = A_2 = 4C_{44}/(C_{11}+C_{33}-2C_{13})$. For the shear anisotropic factor for the $\{001\}$ shear planes between the $\langle 110\rangle$ and $\langle 010\rangle$ directions is expressed by $A_3 = 4C_{66}/(C_{11}+C_{22}-2C_{12})$. For an isotropic crystal, the factors A_1, A_2, and A_3 must be 1.0, while any value smaller or greater than 1.0 is a measure of the degree of elastic anisotropy possessed by the crystal. Using the above relations, A_1, A_2, and A_3 are about 0.777, 0.777, and 1.003, respectively. This indicates that the elastic anisotropy for the $\{001\}$ shear planes between $\langle 110\rangle$ and $\langle 010\rangle$ directions is much smaller than those for the $\{100\}$ shear planes between the $\langle 011\rangle$ and $\langle 010\rangle$ directions and for the $\{010\}$ shear planes between the $\langle 101\rangle$ and $\langle 001\rangle$ directions. Meanwhile, these results also demonstrate that the $\{100\}$ and $\{010\}$ shear planes are easier to be cleavage planes among these principal planes. Moreover, the knowledge of elastic coefficient also provides a method for estimating the anisotropy of linear bulk modulus. The anisotropies of the bulk modulus along the a axis and b axis with respect to the c axis can be estimated by the equations $A_{B_a} = B_a/B_c$ and $A_{B_b} = B_b/B_c$, where B_a, B_b, and B_c are the bulk moduli along different crystal axes and defined as $B_i = idP/di$ ($i = a$, b, and c). Note that a value of one corresponds to the degree of isotropic compressibility and any departure from one represents the degree of anisotropy for the linear compressibility. The A_{B_a} and A_{B_b} of $P\bar{3}m1$-TcB are 0.758 and 0.758, respectively. This indicates that the compressibility along the c axis is lower than those along the a axis and b axis, which agrees well with the calculated elastic constants values of C_{11} and C_{33}.

To understand the mechanical properties on a fundamental level, the total and partial densities of states (DOS) are plotted in Fig. 5. Obviously, the adequately large total DOS at the Fermi level indicates that $P\bar{3}m1$-TcB exhibits a good metallic behavior. This metallicity might make it a better candidate for hard conductors. From partial DOS, one can see that the peaks from -12 eV to -6.8 eV are mainly originated from by B-2s, B-2p, and Tc-4d states with a small contribution from the Tc-4p state. The states from -6.8 eV to 0 eV mainly come from the Tc-4d and B-2p orbitals with slight contributions of Tc-4p and Tc-5s. It is also found that the part DOS profiles of Tc-4d and B-2p are very similar in the range from -6.8 eV to 0, indicating that the Tc-4d orbital has a strong hybridization with the B-2p orbital. This fact also reveals the existence of a strong covalent bonding between the Tc and B atoms. Moreover, the typical feature of the total DOS is the presence of the so-called pseudogap, which is deemed to the borderline between the bonding states and antibonding states. It should be pointed out that the E_F is located below the pseudogap in the $P\bar{3}m1$ phase, reflecting that its bonding states are partially occupied and full antibonding states are unoccupied. This also leads to the high bulk modulus, large shear modulus, and small Poission's ratio (see Table 1).

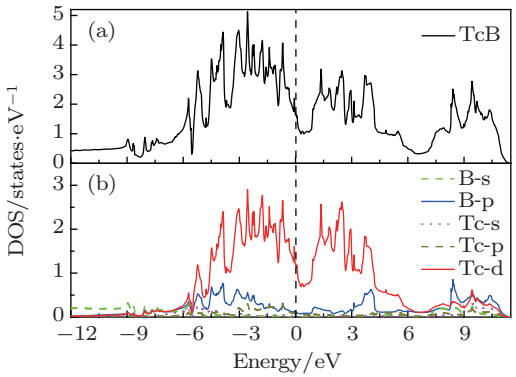


Fig. 5. (color online) Total (a) and partial (b) densities of states (DOS) of $P\bar{3}m1$-TcB. The dashed line denotes the Fermi level E_F.

The investigation on the thermodynamic properties of solids at high pressure and high temperature is an interesting topic in materials science. Thus the thermal properties of $P\bar{3}m1$-TcB are determined in the temperature range from 0 K to 1200 K, in which the quasi-harmonic model remains fully valid,[49] and meanwhile the pressure effect is considered in the range of 0∼50 GPa. Figure 6(a) presents the calculated normalized volume V/V_0 and bulk modulus B of $P\bar{3}m1$-TcB as a function of pressure at different temperatures, respectively. Evidently, the V/V_0 curve becomes steeper with increasing temperature, indicating $P\bar{3}m1$-TcB is compressed more easily at higher temperature. From Fig. 6(b), it can be easily seen that the bulk modulus decreases slightly with temperature at a given pressure and increases monotonously with pressure at

a given temperature, which is in accord with the trend of the volume and also shows that the effect of the pressure on B is much more significant than temperature.

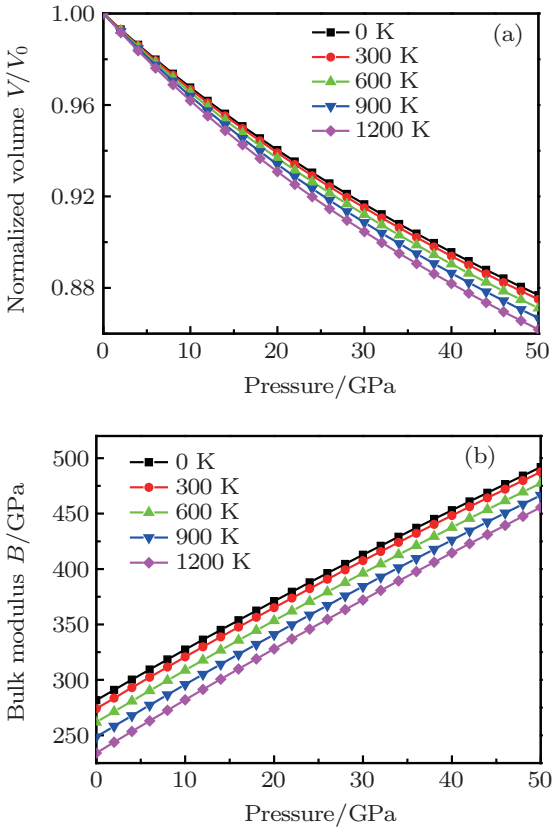


Fig. 6. (color online) Calculated normalized volume V/V_0 (a) and bulk modulus B of $P\bar{3}m1$-TcB (b) as a function of pressure at different temperatures.

Table 2. Calculated Debye temperature Θ (in unit K) and Grüneisen parameter γ of $P\bar{3}m1$-TcB under different pressures and different temperatures.

T/K	P/GPa	0	10	20	30	40	50
0	Θ	720.21	772.79	819.07	860.60	898.40	933.24
	γ	2.210	2.080	1.978	1.896	1.826	1.766
200	Θ	718.07	771.23	817.82	859.57	897.55	932.52
	γ	2.216	2.083	1.981	1.898	1.828	1.767
400	Θ	710.91	765.18	812.71	855.19	893.75	929.17
	γ	2.235	2.097	1.992	1.906	1.835	1.773
600	Θ	701.50	757.49	806.16	849.48	888.70	924.61
	γ	2.261	2.116	2.006	1.917	1.844	1.781
800	Θ	691.54	749.11	798.97	843.19	883.11	919.61
	γ	2.290	2.136	2.021	1.930	1.854	1.789
1000	Θ	680.82	740.20	791.36	836.61	877.25	914.36
	γ	2.321	2.158	2.038	1.943	1.865	1.798
1200	Θ	669.28	730.88	783.49	829.72	871.16	908.85
	γ	2.357	2.182	2.055	1.957	1.876	1.808

As two key thermodynamic quantities: the Debye temperature Θ relates to specific heat, dynamic properties, and melting temperature of solids, and the Grüneisen parameter γ describes the anharmonic effects in the vibrating lattice. The two quantities at various pressures and different temperatures are listed in Table 2. It can be seen clearly from Table 2 that, for a given temperature, Θ increases and γ decreases with increasing pressure. As the applied pressure varies from 0 to 50 GPa, Θ increases by 29.6%, 29.9%, 30.7%, 31.8%, 33%, 34.3%, and 35.8%, and γ decreases by 20%, 20.3%, 20.7%, 21.2%, 21.9%, 22.5%, and 23.3% at temperatures of 0, 200, 400, 600, 800, 1000, and 1200 K, respectively. For a given pressure, Θ decreases and γ increases with increasing temperature. As the applied temperature changes from 0 to 1200 K, Θ decreases by 7.1%, 5.4%, 4.3%, 3.6%, 3%, and 2.6%, and γ increases by 6.7%, 4.9%, 3.9%, 3.2%, 2.7%, and 2.4%, respectively. In addition, it is also found that, for a given temperature, Θ increases linearly and γ decreases almost exponentially especially for high temperature with increasing pressure. As pressure increases, the effects of temperature on them becomes less significant than pressure.

The temperature dependence of the calculated specific heat at constant volume C_V and specific heat at constant pressure C_P at different pressures are investigated, and the results are shown in Fig. 7. At low temperature, the difference of between C_V and C_P is very small, and the increases of C_V and C_P obey the harmonic approximations of the Debye model ($\sim T^3$). However, the anharmonic effect on C_V is suppressed at sufficient high temperature, and C_V is close to a constant value which is called the Dulong–Petit limit ($C_V(T) \sim 3R$ for monoatomic solids), and C_P increases monotonously with the enhancement of the temperature. From Figs. 7(b) and 7(d), it is also found that C_V and C_P decrease with pressure at a given temperature and C_V and C_P increase with temperature at a given pressure, therefore, temperature has a more significant influence on the specific heat than pressure.

The temperature and pressure dependences of the thermal expansion coefficient α are displayed in Fig. 8(a)–8(b), respectively. It can be seen from Fig. 8(a) that α increases steeply at low temperature especially for the case of 0 GPa, then gradually approaches to a linear increase at high temperature, finally becoming gentle at sufficiently high temperature. The influence of pressure on α is relatively small at low temperature, whereas the influence is enhanced obviously at high temperature. As pressure increases, α decreases rapidly at a given temperature and the effect of the temperature on it becomes less marked. From Fig. 8(b), one can also find that α tends to a constant value at high temperature and pressure. All of these results are similar to those of many kinds of materials by the Debye theory, such as ReB_2,[50] OsB_4,[51] $PtAs_2$,[52] and FeB_4.[53]

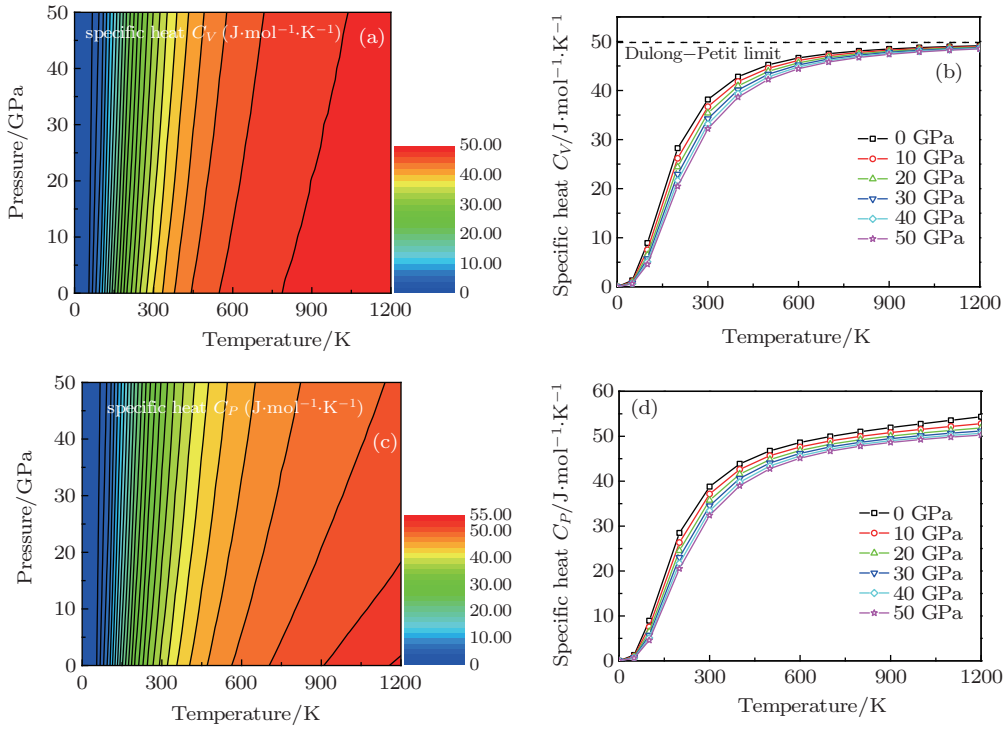


Fig. 7. (color online) Temperature dependence of the calculated specific heat at constant volume C_V and specific heat at constant pressure C_P at different pressures for $P\bar{3}m1$-TcB: (a) C_V contours, (b) C_V–T, (c) C_P contours, and (d) C_P–T.

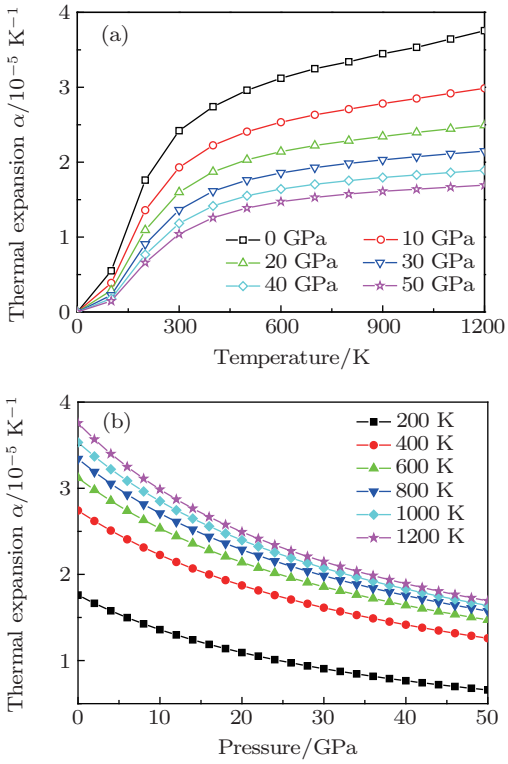


Fig. 8. (color online) (a) Temperature dependence of the thermal expansion coefficient α for $P\bar{3}m1$-TcB at different pressures. (b) Pressure dependence of the thermal expansion coefficient α for $P\bar{3}m1$-TcB at different temperatures.

4. Conclusions

In conclusion, a hexagonal $P\bar{3}m1$ structure is uncovered to be the ground-state structure for TcB by using the PSO algorithm, and it is energetically more preferable than the previously proposed WC-type and *Cmcm* structures. The phonon and formation enthalpy calculations show that the $P\bar{3}m1$ phase is dynamically stable and synthesizable under the ambient condition. The predicted high bulk modulus, large shear modulus, small Poisson's ratio, and considerable hardness reveal that $P\bar{3}m1$-TcB is an ultra-incompressible and hard material. In addition, the investigations of the elastic anisotropic factors suggest that $P\bar{3}m1$-TcB has a certain degree of elastic anisotropy. Detailed analyses of the electronic structure unravel that the strong covalent bonding of Tc–B plays a major role in forming a hard material. By the quasi-harmonic Debye model, the thermodynamic properties, such as the compressibility, bulk modulus, Debye temperature, Grüneisen parameter, specific heat, and thermal expansion coefficient of TcB under high temperature and pressure, are obtained successfully and the corresponding results are also explained. We hope that our theoretical results will stimulate further experimental research on this material in further investigations.

Acknowledgment

We acknowledge Prof. J J Zhao for his critical reading of the manuscript.

References

[1] Occelli F, Farber D L and Toullec R L 2003 *Nat. Mater.* **2** 151
[2] Zhang Y, Sun H and Chen C F 2006 *Phys. Rev. B* **73** 144115

[3] He D W, Zhao Y S, Daemen L, Qian J, Shen T D and Zerda T W 2002 *Appl. Phys. Lett.* **81** 643
[4] Solozhenko V L, Andrault D, Fiquet G, Mezouar M and Rubie D C 2001 *Appl. Phys. Lett.* **78** 1385
[5] Solozhenko V L, Kurakevych O O, Andrault D, Godec Y L and Mezouar M 2009 *Phys. Rev. Lett.* **102** 015506
[6] Cumberland R W, Weinberger M B, Gilman J J, Clark S M, Tolbert S H and R B Kaner 2005 *J. Am. Chem. Soc.* **127** 7264
[7] Chung H Y, Weinberger M B, Levine J B, Kavner A, Yang J M, Tolbert S H and R B Kaner 2007 *Science* **316** 436
[8] Zhang M G, Yan H Y, Zhang G T and Wang H 2012 *Chin. Phys. B* **21** 076103
[9] Zhao W J, Xu H B and Wang Y X 2010 *Chin. Phys. B* **19** 016201
[10] Liang Y C, Guo W L and Fang Z 2007 *Acta Phys. Sin.* **56** 4847 (in Chinese)
[11] Gou H Y, Hou L, Zhang J W, Li H, Sun G F and Gao F M 2006 *Appl. Phys. Lett.* **88** 221904
[12] Chen Z Y, Xiang H J, Yang J L, Hou J G and Zhu Q S 2006 *Phys. Rev. B* **74** 012102
[13] Yang J, Sun H and Chen C 2008 *J. Am. Chem. Soc.* **130** 7200
[14] Young A F, Sanloup C, Gregoryanz E, Scandolo S, Hemley R J and Mao H K 2006 *Phys. Rev. Lett.* **96** 155501
[15] Kempter C P and Nadler M R 1960 *J. Chem. Phys.* **33** 1580
[16] Guo X J, Xu B, He J L, Yu D L, Liu Z Y and Tian Y J 2008 *Appl. Phys. Lett.* **93** 041904
[17] Liang Y C, Zhao J Z and Zhang B 2008 *Solid State Commun.* **146** 450
[18] Zhang M G, Yan H Y, Zhang G T and Wang H 2012 *J. Phys. Chem. C* **116** 4293
[19] Wang Y X 2007 *Appl. Phys. Lett.* **91** 101904
[20] Liang Y C, Li C, Guo W L and Zhang W Q 2009 *Phys. Rev. B* **79** 024111
[21] Aydin S and Simsek M 2009 *Phys, Rev. B* **80** 134107
[22] Deligoz E, Colakoglu K, Ozisik H B and Ciftci Y O 2012 *Solid State Sci.* **14** 794
[23] Zhong M M, Kuang X Y, Wang Z H, Shao P, Ding L P, Huang X F 2013 *J. Phys. Chem. C* **117** 10643
[24] Wu J H and Yang G 2014 *Comp. Mater. Sci.* **82** 86
[25] Li J F, Wang X L, Liu K, Sun Y Y, Chen L and Yang H G 2010 *Physica B* **405** 4659
[26] Wang Y C, Lv J, Zhu L and Ma Y M 2010 *Phys. Rev. B* **82** 094116
[27] Lv J, Wang Y C, Zhu L and Ma Y M 2011 *Phys. Rev. Lett.* **106** 015503
[28] Zhu L, Wang H, Wang Y C, Lv J, Ma Y M, Cui Q L, Ma Y M and Zou G T 2011 *Phys. Rev. Lett.* **106** 145501
[29] Zhao Z S, Xu B, Wang L M, Zhou X F, He J L, Liu Z Y, Wang H T and Tian Y J 2011 *ACS Nano* **5** 7226
[30] Blanco M A, Francisco E and Luaña V 2004 *Comput. Phys. Commun.* **158** 57
[31] Ma Y M, Wang Y C, Lv J and Zhu L http://nlshm-lab.jlu.edu.cn/∼calypso.html
[32] Kohn W and Sham L J 1965 *Phys. Rev. A* **140** 1133
[33] Perdew J P, Burke K and Ernzerhof M 1996 *Phys. Rev. Lett.* **77** 3865
[34] Kresse G and Joubert D 1999 *Phys. Rev. B* **59** 1758
[35] Blöchl P E 1994 *Phys. Rev. B* **50** 17953
[36] Monkhorst H J and Pack J D 1976 *Phys. Rev. B* **13** 5188
[37] Togo A, Oba F and Tanaka I 2008 *Phys. Rev. B* **78** 134106
[38] Hill R 1952 *Proc. Phys. Soc. A* **65** 349
[39] Birch F 1947 *Phys. Rev.* **71** 809
[40] Will G and Kiefer B 2001 *Z. Anorg. Allg. Chem.* **627** 2100
[41] Born M 1940 *Proc. Cambridge Philos. Soc.* **36** 160
[42] Gu Q F, Krauss G and Steurer W 2008 *Adv. Mater.* **20** 3620
[43] Jiang X, Zhao J J and Jiang X 2011 *Comp. Mater. Sci.* **50** 2287
[44] Chen X Q, Niu H Y, Li D Z and Li Y Y 2011 *Intermetallics* **19** 1275
[45] Ravindran P, Fast L, Korzhavyi P A, Johansson B, Wills J and Eriksson O 1998 *J. Appl. Phys.* **84** 4891
[46] Hao X F, Xu Y H, Wu Z J, Zhou D F, Liu X J and Meng J 2008 *J. Alloys Compd.* **453** 413
[47] Li Y L and Zeng Z 2009 *Chem. Phys. Lett.* **474** 93
[48] Hao X F, Xu Y H, Wu Z J, Zhou D F, Liu X J, Cao X Q and Meng J 2006 *Phys. Rev. B* **74** 224112
[49] Johnston W D, Miller R C and Damon D H 1965 *J. Less-Common Met.* **8** 272
[50] Peng F, Liu Q, Fu H Z and Yang X D 2009 *Solid State Commun.* **149** 56
[51] Yan H Y, Zhang M G, Huang D H and Wei Q 2013 *Solid State Sci.* **18** 17
[52] Yan H Y and Zhang M G 2014 *Comp. Mater. Sci.* **86** 124
[53] Zhang X Y, Qin J Q, Ning J L, Sun X W, Li X T, Ma M Z and Liu R P 2013 *J. Appl. Phys.* **114** 183517